Steady State Analysis of Squirrel-Cage Induction Machine with Skin-Effect

Dr.-Ing. O. I. Okoro

Department of Electrical Engineering
University of Nigeria, Nsukka
Enugu State, Nigeria.
Email: ogbonnayaokoro@hotmail.com

ABSTRACT

The Steady state analysis of a rectangular shaped-rotor type squirrel-cage induction machine was examined numerically with the help of MATLAB®. The results of the proposed Skin-effect model were compared with the conventional model. The results of this comparison show that a large error occurs when the influence of skin-effect is neglected in the analysis of a squirrel-cage induction machine at high rotor frequency.

(Key words: squirrel-cage, induction machine, steady state, skin effect, conventional model, rectangular rotor bar)

INTRODUCTION

The transient state model or the steady-state equivalent circuit is usually employed to represent an induction machine. Generally, the steady-state equivalent circuit is used when the machine is running at steady-state, and a transient state model is used when the machine is running at transient operations. Unfortunately, the conventional model of an induction machine, which consists of an equivalent circuit with a single loop, is not adequate to take into account the skin-effect in rotor bars; which may not be negligible when the machine is fed from non-sinusoidal voltage or current source [1,2].

Pertinently, for the study of skin-effect in rotor bars, the rotor circuit needs to be modified in order to adequately take into account the wide range of frequencies occurring in the machine. Levy [3] and Creer [4] have proposed a rotor model with three rotor loops. It has been noted by [2] that the model accuracy increases when the number of the rotor loops is increased to four or more. In this paper, the rotor circuit is modeled as proposed by [2].

This paper highlights the method used for the identification of the rotor circuit parameters. This paper also includes the development of the mathematical analysis for the steady-state conventional and skin-effect models. The paper concludes with a computer simulation and some relevant comments on the results.

ROTOR CIRCUIT PARAMETER IDENTIFICATION

The test machine used in this study is a KATT VDE 0530, Class F insulation, surfaced-cooled Squirrel-cage induction motor. The rated power, speed, and current are 7.5KW, 1400rpm, and 19.2A, respectively. Figure 1 shows the test machine. The slot geometry, showing the stator and rotor shapes, is shown in Figure 2.

Figure 1: The 7.5KW test motor.

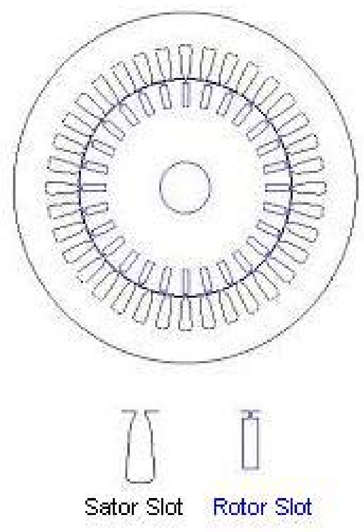

Figure 2: Slot geometry of the test machine.

To model the rotor bar, a T-configuration network is used according to the method proposed by Babb and Williams [5]. The rotor bar is divided into five sections as shown in Figure 3.

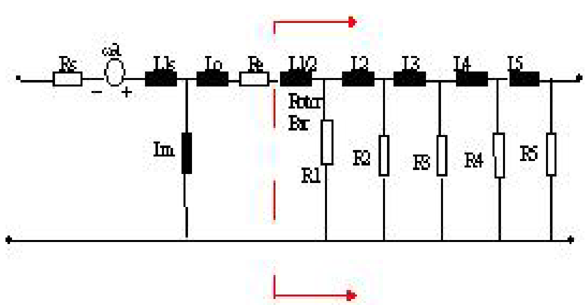

Figure 3: Equivalent T-Circuit; Configuration for 5-section rotor bar.

The rotor bar resistance and inductance for each section is,

$$R_{\sec} = \frac{L_s}{\chi_{cu} h_{\sec} b_{Nut}} \quad (1)$$

$$L_{\sec} = \frac{\mu_o L_s h_{\sec}}{b_{Nut}} \quad (2)$$

where,

μ_o = Permeability of free space
b_{Nut} = Width of the rotor bar
h_{sec} = height of each bar section
χ_{cu} = conductivity of copper conductor
L_s = Length of rotor bar

It is important to note, that equations (1) and (2) are modified to account for all of the bars and are subsequently referred to the stator by using the transformation factor, K. The values of the referred rotor inductances and resistances are defined mathematically by,

$$L1r = k^2 L10 \quad (3a)$$

$$L2r = k^2 L2 \quad (3b)$$

$$L3r = k^2 L3 \quad (3c)$$

$$L4r = k^2 L4 \quad (3d)$$

$$L5r = k^2 L5 \quad (3e)$$

$$L10 = Lo + L1/2 \quad (3f)$$

$$\mathrm{Re}\, r = k^2 \mathrm{Re} \quad (4a)$$

$$R1r = k^2 R1 \quad (4b)$$

$$R2r = k^2 R2 \quad (4c)$$

$$R3r = k^2 R3 \quad (4d)$$

$$R4r = k^2 R4 \quad (4e)$$

$$R5r = k^2 R5 \quad (4f)$$

where k_1 is defined thus [6]:

$$k_1^{\ 2} = \frac{m1}{m2}\left(\frac{k_{w1} N1}{k_{w2} N2}\right)^2 \quad (5)$$

where,
m1 = number of phases on the stator
m2 = number of phases on the rotor
k_{w1} = stator winding factor

k_{w2} = rotor winding factor
N1 = number of series-connected turns per phase of the stator
N2 = number of series-connected turns per phase of the rotor

But, m2 = (number of rotor bars)/(number of pairs of poles)

$$m2 = \frac{Q}{P} \quad (6)$$

Seinsch [7] defines the relationship between the rotor bar resistance and the rotor resistance as:

$$R_2 = \frac{R_{bar}}{P} \quad (7)$$

with the equivalent rotor referred resistance as,

$$R'2 = k^2 R_{bar} \quad (8)$$

where,

$$k^2 = \frac{k_1^{\,2}}{P} \quad (9)$$

By using the optimization technique reported in [2], the values of the rotor circuit parameters can be found at 4KHz rotor frequency. The result of the optimization, as shown in Figure 4, closely matches with the actual rotor bar characteristics of the machine. At approximately 4KHz frequency, the error in the developed rotor model is about 6%. Table 1 shows the estimated rotor circuit parameters.

CONVENTIONAL AND SKIN EFFECT STEADY STATE ANALYSIS

For the purpose of digital simulation, the electrical model of the squirrel-cage induction machine can be represented in state variable form with currents as state variables by equation (10).

$$\frac{d[\mathbf{i}]}{dt} = -[\mathbf{L}]^{-1}([\mathbf{R}] + \omega_r[\mathbf{G}])[\mathbf{i}] + [\mathbf{L}]^{-1}[\mathbf{V}] \quad (10)$$

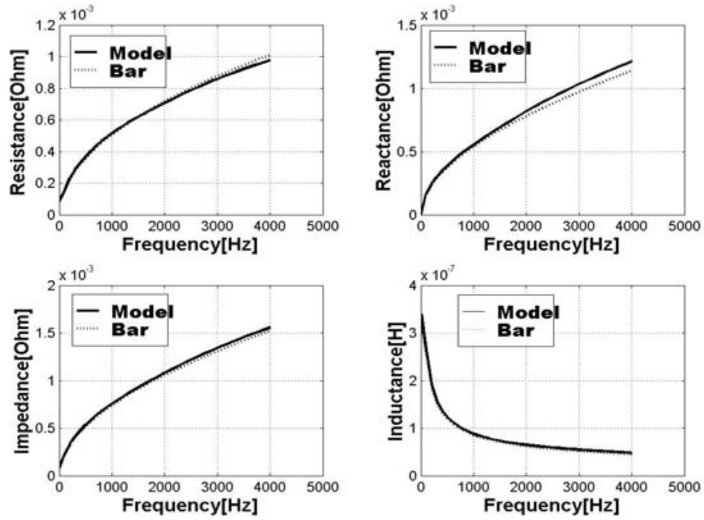

Figure 4: Model Plots for Bar Sections (100) and Model Sections (5).

Table1: Computed Model Impedance at 4KHz.

Resistance	[mΩ]	Inductance	[μH]
R_1	1.338	L_1	6.1150e-2
R_2	0.656	L_2	9.2940e-2
R_3	0.321	L_3	0.1896
R_4	0.179	L_4	0.3562
R_5	1.338	L_5	0.2596

In consideration of the steady-state equation of the induction machine with skin-effect, the time derivatives of current in equation (10) are set to zero, with the rotor speed constant, and the machine d- and q-voltages and currents are referred to the synchronously rotating reference frame. By so doing, the resultant algebraic equation can be expressed in compact form as:

$$[\mathbf{V_o}] = [\mathbf{Z_o}][\mathbf{I_o}] \quad (11)$$

and,

$$\mathbf{I}o = [\mathbf{Z_o}]^{-1}[\mathbf{V_o}] \quad (12)$$

For the conventional steady- state model:

$$[\mathbf{I}_o]=[\mathbf{I}_{qso} \quad \mathbf{I}_{dso} \quad \mathbf{I}_{qro} \quad \mathbf{I}_{dro}]^t \text{ ———— } (13)$$

$$[\mathbf{V}_o]=[\mathbf{V}_{qso} \quad \mathbf{V}_{dso} \quad 0 \quad 0]^t \text{ ———— } (14)$$

and,

$$[\mathbf{Z}_o]=\begin{bmatrix} R_s & \omega_b L_s & 0 & \omega_b L_m \\ -\omega_b L_s & R_s & -\omega_b L_m & 0 \\ 0 & (\omega_b-\omega_r)L_m & R_r & (\omega_b-\omega_r)L_r \\ -(\omega_b-\omega_r)L_m & 0 & -(\omega_b-\omega_r)L_r & R_r \end{bmatrix}$$

(15)

For the skin-effect steady-state model, we have:

$$\mathbf{I}_o=[id_{so} \quad iq_{so} \quad iD1o \quad iQ1o \quad iD2o \quad iQ2o \quad iD3o \quad iQ3o \quad iD4o \quad iQ4o \quad iD5o \quad iQ5o]^t \text{ ——— } (16)$$

$$[\mathbf{V_o}]=[Vd_{so} \quad Vq_{so} \quad 0 \quad 0 \quad 0 \quad 0 \quad 0 \quad 0 \quad 0 \quad 0 \quad 0 \quad 0]^t \ (17)$$

and,

$$[\mathbf{Z_o}]=\begin{bmatrix} Rs & -Ls\omega_b & 0 & -Lm\omega_b & 0 & 0 & 0 & 0 & 0 & 0 & 0 & 0 \\ Ls\omega_b & Rs & Lm\omega_b & 0 & 0 & 0 & 0 & 0 & 0 & 0 & 0 & 0 \\ 0 & (\omega_r-\omega_b)Lm & R11 & (\omega_r-\omega_b)Lr & -R1r & 0 & 0 & 0 & 0 & 0 & 0 & 0 \\ (\omega_b-\omega_r)Lm & 0 & (\omega_b-\omega_r)Lr & R11 & 0 & -R1r & 0 & 0 & 0 & 0 & 0 & 0 \\ 0 & 0 & -R1r & 0 & R22 & 0 & -R2r & 0 & 0 & 0 & 0 & 0 \\ 0 & 0 & 0 & -R1r & 0 & R22 & 0 & -R2r & 0 & 0 & 0 & 0 \\ 0 & 0 & 0 & 0 & -R2r & 0 & R33 & 0 & -R3r & 0 & 0 & 0 \\ 0 & 0 & 0 & 0 & 0 & -R2r & 0 & R33 & 0 & -R3r & 0 & 0 \\ 0 & 0 & 0 & 0 & 0 & 0 & -R3r & 0 & R44 & 0 & -R4r & 0 \\ 0 & 0 & 0 & 0 & 0 & 0 & 0 & -R3r & 0 & R44 & 0 & -R4r \\ 0 & 0 & 0 & 0 & 0 & 0 & 0 & 0 & -R4r & 0 & R55 & 0 \\ 0 & 0 & 0 & 0 & 0 & 0 & 0 & 0 & 0 & -R4r & 0 & R55 \end{bmatrix}$$

(18)

$$R11 = \mathrm{Re}r + R1r \text{ ———————— } (19a)$$

$$R22 = R1r + R2r \text{ ———————— } (19b)$$

$$R33 = R2r + R3r \text{ ———————— } (19c)$$

$$R44 = R3r + R4r \text{ ———————— } (19d)$$

$$R55 = R4r + R5r \text{ ———————— } (19e)$$

$$\omega_b = 2\pi f \text{ ———————— } (19f)$$

where,

V_{qso} = Steady-state q-axis stator voltage
V_{dso} = Steady-state d-axis stator voltage
i_{qso}, i_{dso} = Steady-state q- and d-axis stator currents, respectively
i_{qro}, i_{dro} = Steady-state q- and d-axis rotor currents, respectively
I_{qro}, I_{dro} = Steady-state q- and d-axis rotor currents, respectively
I_{Q1o}, I_{Q2o} = Steady-state q-axis rotor currents in loop1 and loop2, respectively
I_{D1o}, I_{D2o} = Steady-state d-axis rotor currents in loop1 and loop2, respectively
f = Rated frequency

The electromagnetic behavior of the machine under steady-state condition is described by the equation:

$$T_{eo} = 1.5PL_m\left(i_{qso}i_{dro} - i_{dso}i_{qro}\right) \text{ ——— } (20)$$

where,

T_{eo} = Steady-state electromagnetic torque
L_m = Magnetizing inductance
P = Number of pole pairs.

RESULTS AND DISCUSSION

MATLAB m-files [8] were developed and used to solve equations (12) and (20), for both the conventional and skin-effect steady-state analysis. The developed program accepts constant stator and rotor quantities, such as resistances and inductances as inputs.

These constant quantities were found through the open-circuit test, blocked-rotor test, and D.C. measurement test, carried out on the 7.5KW Squirrel-cage induction machine. The machine data is shown in Appendix A. By supplying these input parameters, the steady-state behaviour of the machine can be predicted. The graphical representations for stator current, input power, output power, torque, efficiency, and power factor as a function of mechanical rotor speed are shown in Figure 5 and Figure 6 for the conventional and skin-effect analysis respectively.

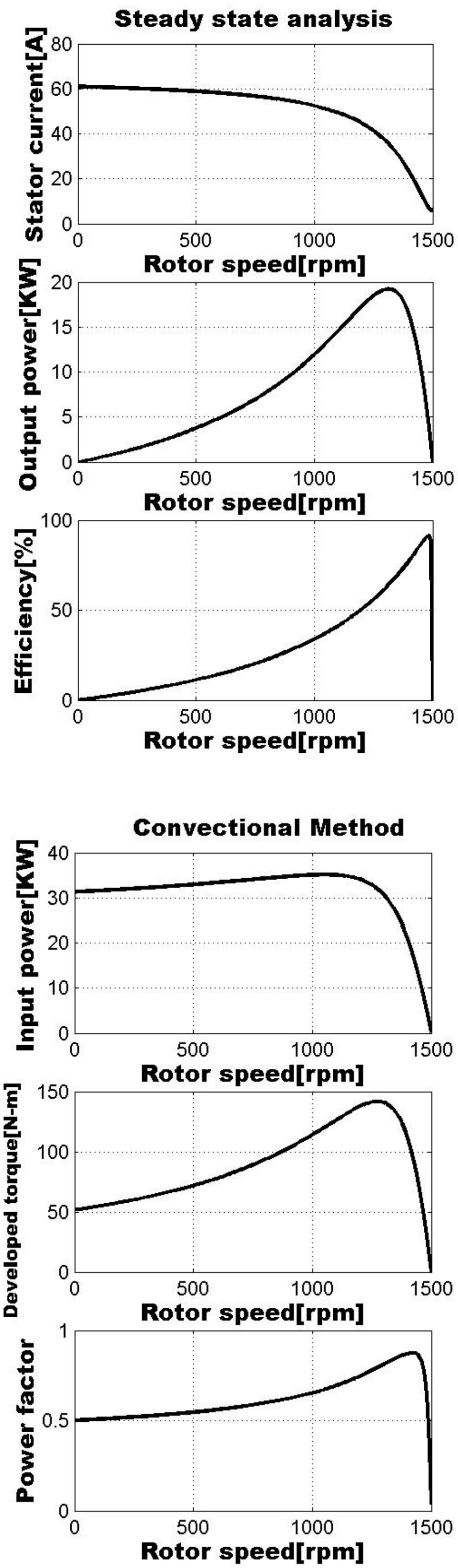

Figure 5: Steady State Performance Curves (Conventional Model)

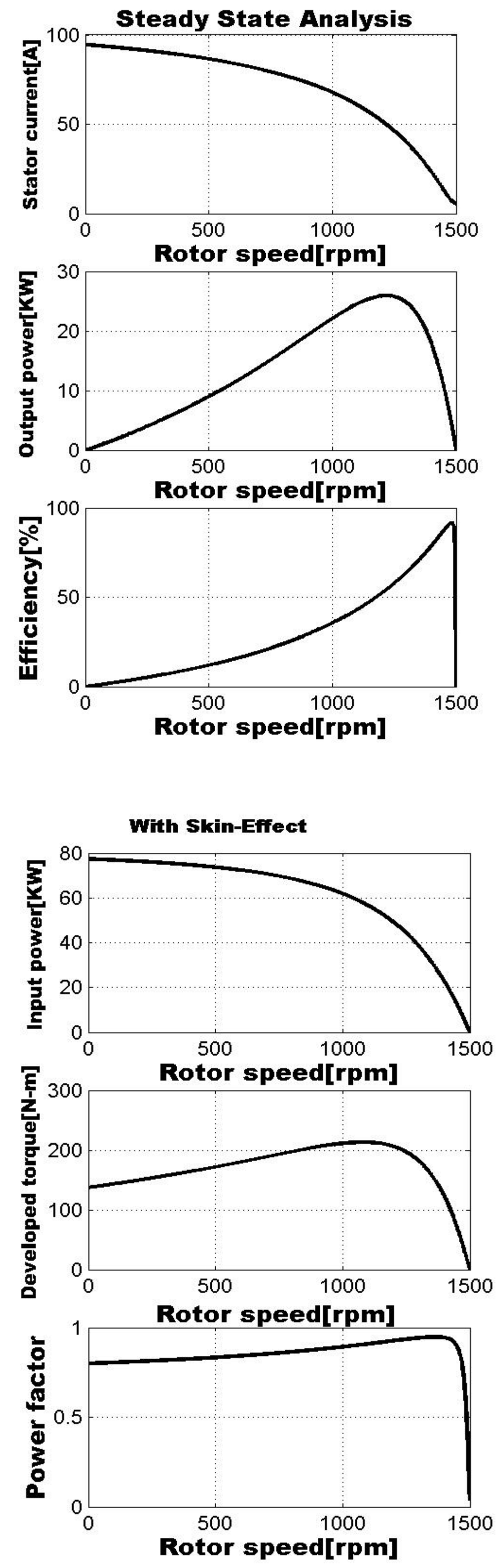

Figure 6: Steady State Performance Curves (Skin-Effect Model)

In order to visualise the effects of skin effect on the steady and transient states performances of the induction machine, the results of the simulation involving skin-effect have to be compared graphically with that from the conventional model in Figure 7.

The steady-state magnitude of the rotor bar currents for each section, as a function of mechanical rotor speed, is shown in Figure 8. From Figure 8, it can be seen that as the bar depth increases, the magnitude of the rotor bar current decreases. This explains why higher current flows through the first rotor bar section as opposed to the other sections at starting.

CONCULSIONS

The paper has systematically presented the steady-state analysis of Squirrel-cage induction machine with skin-effect. The simulated results indicate that there exists a significant difference between the conventional steady-state model, and the steady-state model with skin-effect.

The developed torque in the skin-effect machine model was about three times greater than that of the conventional machine model at starting. Additionally, at starting, the magnitude of the stator current, power factor, and input power of the skin-effect model was observed to be higher than that of the conventional model.

From the results presented in this paper, it can be seen that at high rotor frequency, the conventional machine model fails to predict accurately the steady-state behaviour of the machine. The results presented in this paper will therefore, form a veritable tool for an industrial engineer in predicting the actual behaviour of a deep-bar Squirrel-cage induction machine prior to design.

ACKNOWLEDGEMENT

The author wishes to express his thanks to DAAD for their financial support and to Prof. Dr.-Ing. B. Weidemann of the University of Kassel, Germany for his assistance and advice in producing this paper.

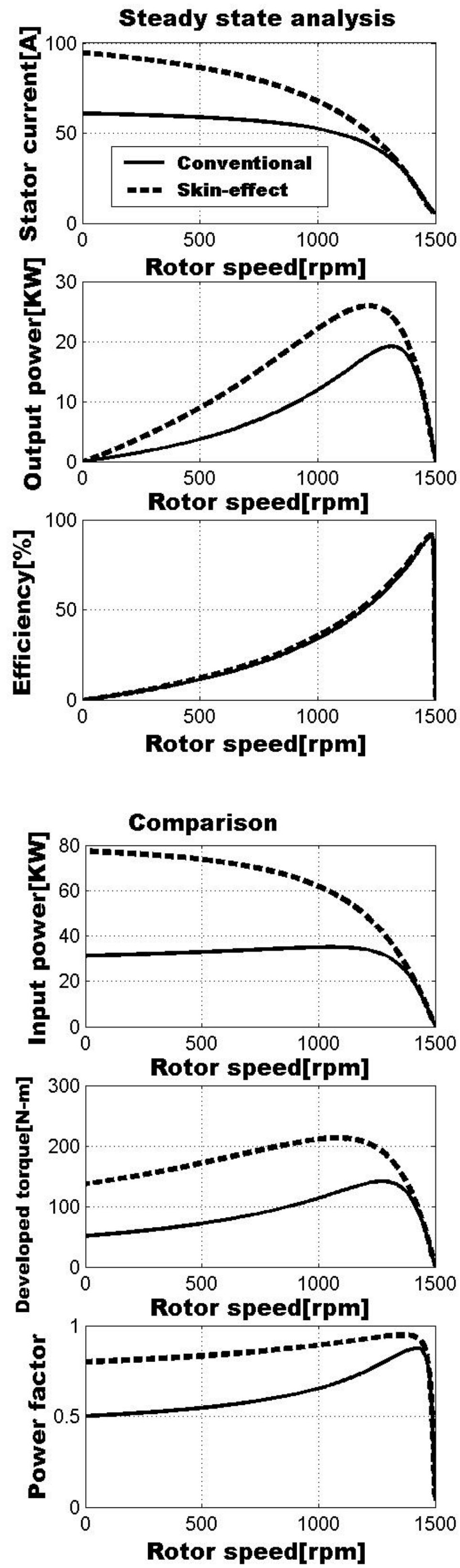

Figure 7: Conventional and Skin-Effect Models Comparison

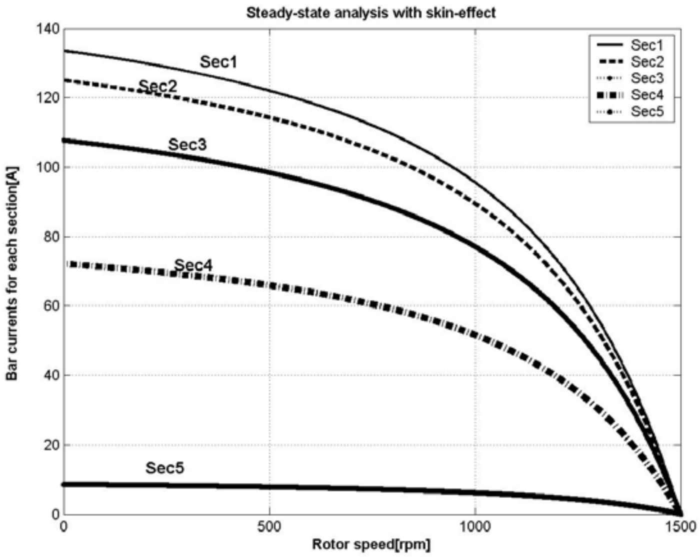

Figure 8: Rotor Bar Currents for each Section with Skin-Effect

APPENDIX A:

Output Power	7.5KW
Rated voltage	340V
Winding connection	Delta
Number of Poles	4
Rated speed	1400rpm
Rated frequency	50Hz
Stator resistance	2.52195ohm
Stator leakage reactance	1.95145ohm
Rotor resistance	0.976292ohm
Rotor leakage reactance	2.99451ohm
Magnetizing reactance	55.3431ohm
Mechanical shaft torque	51.2636N.m
Estimated rotor inertia moment	0.117393Kgm^2
Rated current	19.2A
Moment of inertia of the D.C. motor	0.10958Kgm^2
Shaft stiffness constant	14320Nm/rad

REFERENCES

[1.] DellA'quila, A and L. Salvatore. 1983. Modeling of Inverter-fed Induction Motors by FFT Processing of Voltage and Current Signals. IMACS. 135-143.

[2.] Okoro, O.I. 2002. Dynamic and Thermal Modeling of Induction Machine with Non-Linear Effects. Dissertation. University of Kassel, Germany.

[3.] Levy, W., C.F. Landy, and M.D. McCulloch. 1990. Improved Models for the Simulation of Deep Bar Induction Motors. IEEE Transactions on Energy Conversion. 5(2):393-400.

[4.] Creer, W. H., D.W. Novotny, and T.A. Lipo. 1985. Determination of Equivalent Circuits for Induction Machines with Skin-Effect Using Terminal Characteristics. Electric Machines and Power Systems. 10(5-6):379-394.

[5.] Babb, D.S. and J.E. Williams. 1951. Network Analysis of A-C Machine Conductors. AIEE Transactions. 70:2001-2005.

[6.] Nasar, S.A. and L.E. Unnewehr. 1979. Electromechanics and Electric Machines. John Wiley and Sons: New York.

[7.] Seinsch, H. O. 1988. Grundlagen Elektrischer Maschinen und Antriebe. Teubner: Stuttgart, Germany.

[8.] Mathworks, Inc. 1997. MATLAB User's Guide. The Mathworks, Inc: Natick, New York.

ABOUT THE AUTHOR

Dr.–Ing. O.I. Okoro holds a Ph.D. in Electrical Machines from the University of Kassel, Germany where he conducted his research under a DAAD Scholarship. He currently lectures in the Department of Electrical Engineering at the University of Nigeria, Nsukka. His research interests are in the areas of dynamic simulation and control of induction machines as well as in the thermal and dynamic analysis of AC machines. He is a member of the IEEE.

SUGGESTED CITATION

Okoro, O.I. 2004. Steady State Analysis of Squirrel-Cage Induction Machine with Skin-Effect. *Pacific Journal of Science and Technology*. 5(2):56-62.

Pacific Journal of Science and Technology